


A stable, power scaling, graphene-mode-locked all-fiber oscillator

Cite as: Appl. Phys. Lett. **110**, 243102 (2017); <https://doi.org/10.1063/1.4985293>

Submitted: 24 February 2017 . Accepted: 28 May 2017 . Published Online: 12 June 2017

D. Popa , Z. Jiang, G. E. Bonacchini, Z. Zhao, L. Lombardi, F. Torrisi, A. K. Ott, E. Lidorikis, and A. C. Ferrari



View Online



Export Citation



CrossMark

ARTICLES YOU MAY BE INTERESTED IN

[Sub 200 fs pulse generation from a graphene mode-locked fiber laser](#)

Applied Physics Letters **97**, 203106 (2010); <https://doi.org/10.1063/1.3517251>

[Graphene mode locked, wavelength-tunable, dissipative soliton fiber laser](#)

Applied Physics Letters **96**, 111112 (2010); <https://doi.org/10.1063/1.3367743>

[Few-cycle pulses from a graphene mode-locked all-fiber laser](#)

Applied Physics Letters **106**, 253101 (2015); <https://doi.org/10.1063/1.4922397>

Applied Physics Letters

Mid-IR and THz frequency combs
special collection

[Read Now!](#)



A stable, power scaling, graphene-mode-locked all-fiber oscillator

D. Popa,^{1,a)} Z. Jiang,¹ G. E. Bonacchini,¹ Z. Zhao,¹ L. Lombardi,¹ F. Torrisi,¹ A. K. Ott,¹
 E. Lidorikis,² and A. C. Ferrari¹

¹Cambridge Graphene Centre, University of Cambridge, Cambridge CB3 0FA, United Kingdom

²Department of Materials Science and Engineering, University of Ioannina, Ioannina 45110, Greece

(Received 24 February 2017; accepted 28 May 2017; published online 12 June 2017)

We report power tunability in a fiber laser mode-locked with a solution-processed filtered graphene film on a fiber connector. ~ 370 fs pulses are generated with output power continuously tunable from ~ 4 up to ~ 52 mW. This is a simple, low-cost, compact, portable, all-fiber ultrafast source for applications requiring environmentally stable, portable sources, such as imaging. *Published by AIP Publishing.*
[\[http://dx.doi.org/10.1063/1.4985293\]](http://dx.doi.org/10.1063/1.4985293)

Optical pulses generated by mode-locked lasers are increasingly used in a variety of applications, supporting developments in many scientific, commercial, and industrial areas.^{1,2} The success of lasers in this field is partly fueled by their ability to generate pulses matching various use needs.^{1–5} In medicine, depending on the particular application (e.g., surgery² or imaging^{4,5}), optical pulses operating at specific wavelengths are needed to fit the absorption and scattering profile of a tissue.⁶ For example, in tissue imaging,^{4,5} wavelengths in the ~ 1 – 1.5 μm range minimize photodamage and maximize penetration depth.^{1–5} Similarly, the pulse duration specifies the type of laser-tissue interaction that may occur,^{1–5} while the pulse repetition rate controls the interaction speed.^{1–5} Ultimately, the optical power delivered to the sample needs to balance the desired laser-tissue interaction with any non-desired, e.g., photodamage, effects.^{1–3} For example, in nonlinear microscopy lasers with high, \sim kW level, peak powers are used to generate nonlinear signals of interest while keeping the average power at a few 10s mWs, i.e., below the sample photodamage threshold.^{1,3,5} An important goal is to enable real-time imaging in the operating room or outpatient setting,^{3,4} requiring compact and stable light sources.^{1,3,4} Commercially available solid-state lasers, such as titanium-sapphire (Ti:Sa) pumping optical parametric oscillators (OPOs), can provide a 700–4000 nm tuning range with several 100 mWs average power.⁷ However, both are complex and expensive systems, relying on bulk optics.¹ This has driven a research effort to find novel approaches, not only capable of producing short pulses, but also cheaper, simpler, broadband, and stable. Fiber lasers are attractive platforms for short pulse generation due to their simple and compact designs,⁸ efficient heat dissipation,² and alignment-free operation.^{1,2} These characteristics, combined with advances in glass technology^{9,10} and nonlinear optics¹¹ resulted in systems working from the visible to the mid-infrared.⁹ In fiber oscillators, ultrashort pulses can be obtained by passive mode-locking. This typically requires the aid of a non-linear component called a saturable absorber (SA).^{1,8} Graphene^{12,13} and carbon nanotubes (CNTs)^{12,14–18} have emerged as promising SAs for ultrafast lasers.^{13–30} In CNTs, broadband operation is achieved by

using a distribution of tube diameters,^{17,20} while this is an intrinsic property of graphene.³² This, along with the ultrafast recovery time,³³ low saturation fluence,^{13,31} environmental stability,²⁹ and ease of fabrication,³⁴ and integration,³⁵ makes graphene an excellent broadband SA.³² Consequently, mode-locked lasers using graphene SAs (GSAs) have been demonstrated from ~ 800 nm³⁶ to ~ 970 nm,³⁷ ~ 1 μm ,³⁸ ~ 1.5 μm ,³¹ ~ 2 μm ,³⁹ and ~ 2.4 μm ⁴⁰ up to ~ 2.8 μm .⁴¹ Various approaches have been used to prepare GSAs for mode-locked fiber oscillators with output powers greater than 10 mW, as required for laser imaging.^{1,3} For example, dispersions produced by liquid phase exfoliation (LPE) of graphite⁴² were used to generate ~ 60 mW at 1.1 μm ,⁴³ and ~ 15 mW at 1.5 μm .⁴⁴ Films grown by chemical vapor deposition (CVD) with 1 layer,⁴⁵ 1–2 layers,⁴⁶ and several layers^{47,48} were used to generate ~ 115 mW at 2 μm ,⁴⁵ ~ 15 mW at 1.5 μm ,⁴⁶ ~ 44 mW at 2 μm ,⁴⁷ and ~ 174 mW at 1.5 μm .⁴⁸ Graphene oxide (GO) was also used as an SA, to generate ~ 148 mW at 1 μm ,⁴⁹ and ~ 80 mW at 1.5 μm .⁵⁰ However, GO is an insulating material with many defects and gap states⁵¹ and may not offer the wideband tunability of GSAs. Flakes grown by CVD require high substrate temperatures,³⁵ followed by transfer to the target substrate.³⁵ LPE has the advantage of scalability, room temperature processing, and high yield, and does not require any substrate.³⁵ Dispersions produced by LPE can be easily integrated into various systems.^{34,35}

Here, we use a LPE polymer-free graphene film coated on a fiber based connector as SA. Based on this, we demonstrate mode-locking of an all-fiber laser, achieving stable pulses with ~ 370 fs in duration over a continuous output power tuning range from ~ 3.5 to ~ 52 mW. This enables simple and robust light sources for applications such as laser imaging,³ with adjustable output power and no need of amplification stages.

The GSA is prepared and characterized as described in Ref. 38. Graphite (Sigma Aldrich) is exfoliated via ultrasonic treatment in a solution of deionised water and sodium cholate (0.9 wt. %),^{13,52} followed by ultracentrifugation at 10 000 rpm for 1 h. The resulting 70% top dispersion is then filtered in vacuum through a nitrocellulose membrane (Millipore 100 nm pore-size filter). This blocks the flakes, while allowing water to pass through, resulting in a film on

^{a)}Electronic mail: dp387@cam.ac.uk

the top of the membrane. The film is then placed onto the tip of a fiber connector for physical contact (FC/PC), to be used in the laser, and on a quartz plate, for optical characterization, by applying pressure and heat ($\sim 90^\circ\text{C}$, to improve adhesion) for 1 h, followed by dissolution of the filter in acetone.

To monitor the film quality after filtration, we characterize it by Raman Spectroscopy at 457, 514, and 633 nm, using a Renishaw InVia micro-Raman spectrometer. Figure 1(a) plots a typical Raman spectrum (black curve) of representative flakes of the LPE dispersion on Si/SiO₂.³⁸ Besides the G and 2D peaks, significant D and D' bands as well as their combination mode D + D' at $\sim 2950\text{ cm}^{-1}$ are presented.⁵³ The D and D' peaks are assigned to the sub-micrometer edges of our flakes,⁵⁴ rather than to disorder within the flakes,⁵⁴ also supported by low Disp(G) $\sim 0.05\text{ cm}^{-1}/\text{nm}$,⁵⁵ much lower than in disordered carbons.⁵⁶ Fig. 1(a) plots the Raman spectrum (red curve) of the film on the FC/PC tip, with Disp(G) $\sim 0.02\text{ cm}^{-1}/\text{nm}$. The full width at half maximum of the 2D peak, FWHM(2D), is $\sim 17\text{ cm}^{-1}$ larger than that of the LPE dispersion. However, the 2D peak is still Lorentzian; thus, even if the flakes are multi-layers, they are electronically decoupled and, to a first approximation,

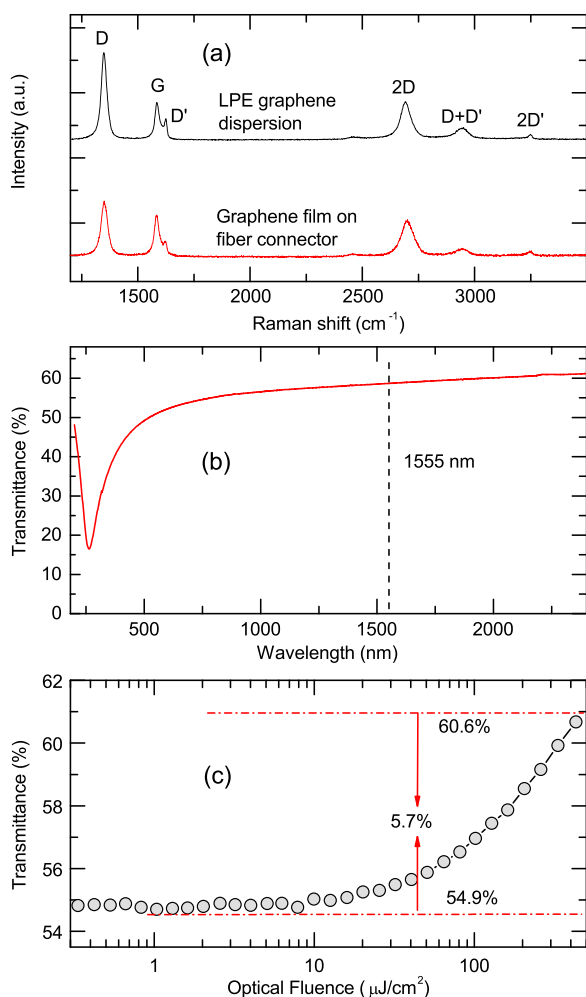


FIG. 1. (a) Raman spectra of film and LPE graphene dispersion. (b) Linear transmittance of film, showing featureless behavior from ~ 500 to $\sim 2400\text{ nm}$. The dip at $\sim 266\text{ nm}$ is due to the van Hove singularity in the graphene density of states.⁵⁸ The laser operating wavelength is marked. (c) Non-linear transmittance at the laser operating wavelength.

behave as a collection of single layers.⁵⁷ We conclude that the filtration does not affect the structure of the flakes in our film.

Figure 1(b) plots the GSA transmittance. Except for the peak at $\sim 266\text{ nm}$, a signature of the van Hove singularity in the graphene density of states,⁵⁸ the spectrum has a featureless linear transmission from ~ 500 to $\sim 2400\text{ nm}$. The transmittance and absorption at 1555 nm (the laser wavelength) are $\sim 59\%$ and $\sim 30\%$, respectively. Reference 38 used the transfer matrix formalism⁵⁹ to estimate the number of graphene layers (N). We apply this formalism and calculate, as a function of N , the absorption of our GSA. In this model, the film is approximated as a multilayered graphene on a quartz substrate. The overall absorption is calculated by evaluating the contributions of multiple reflections. By comparing our calculations with the data at 1555 nm, we estimate that a 30% absorption translates to $N \sim 35\text{--}40$ layers.

The nonlinear optical transmittance is measured with an OPO (Coherent, Chameleon) delivering $\sim 570\text{ fs}$ pulses with 4 MHz repetition rate at 1555 nm. The optical transmittance is determined by monitoring the input and output power [Fig. 1(c)]. The transmittance increases from $\sim 54.9\%$ to $\sim 60.6\%$, a change of $\sim 5.7\%$, suitable for mode-locking of fiber lasers,⁶⁰ that typically operate with higher gain and cavity losses⁸ than their solid-state counterparts.⁶¹

For our oscillator, we design a dispersion-managed soliton laser, able to support higher pulse energies than soliton lasers,^{19,22,31} as shown in Fig. 2, with a total cavity length of $\sim 8\text{ m}$. We use a $\sim 2.3\text{ m}$ erbium doped fiber (EDF), with a second-order dispersion coefficient $\beta^{(2)} \sim 22\text{ ps}^2/\text{km}$ as gain medium. The EDF is pumped by a 980 nm continuous wave (CW) laser diode (LD) through a fused wavelength division multiplexer (WDM). The rest of the cavity is formed from two lengths of standard single mode fiber (SMF): $\sim 5.3\text{ m}$ of SMF-28 with $\beta^{(2)} \sim -22\text{ ps}^2/\text{km}$, and $\sim 0.4\text{ m}$ of Flexcore-1060 with $\beta^{(2)} \sim -7\text{ ps}^2/\text{km}$. This gives a net intracavity second-order dispersion $\sim -0.07\text{ ps}^2$, typical of dispersion-managed soliton lasers.^{19,22,31} Unidirectional propagation is ensured by an optical isolator (ISO). A polarization controller (PC) is used for mode-locking optimization and stabilization. In order to reduce the effects that high power injected in the fiber could have on graphene⁶² and its stability, the output of the laser is provided by the 70% port of a 70/30 output coupler (OC). Mode-locking starts at $\sim 28\text{ mW}$ pump power, with output power $P_{out} \sim 3.7\text{ mW}$. The average P_{out}

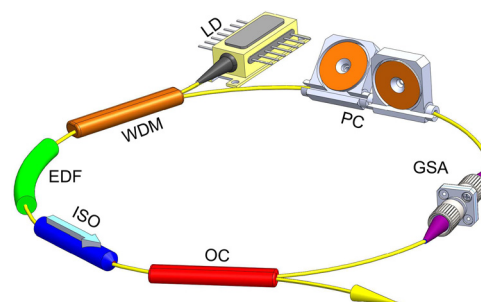


FIG. 2. Laser schematic. LD: Laser diode; WDM: Wavelength division multiplexer; EDF: Erbium doped fiber; ISO: Isolator; OC: Optical coupler; PC: Polarization controller.

then scales linearly with pump power as in Fig. 3(a), with a maximum $P_{out} \sim 52$ mW at 232 mW pump. For this power range, we measure a maximum $\sim 367 \pm 8$ fs variation in the pulse duration, as shown in Fig. 3(a). The pulse optical spectrum plotted in Fig. 3(b), with $\Delta\lambda = 8.2$ nm spectral width, exhibits sidebands related to a periodic disturbance of soliton pulses in the laser resonator,^{1,2} as expected for soliton operation in fiber lasers.¹ Removing the GSA results in CW operation of the laser [Fig. 3(b), red line]. The corresponding intensity autocorrelation trace, pedestal free, is shown in Fig. 3(c), with $\Delta\tau = 364$ fs pulse duration, as determined by fitting a $sech^2$ profile to the pulse, as expected for soliton-like mode-locking.⁶³ This gives a time bandwidth product $\Delta\nu\Delta\tau = 0.37$, close to the expected transform limit 0.315.⁶⁴

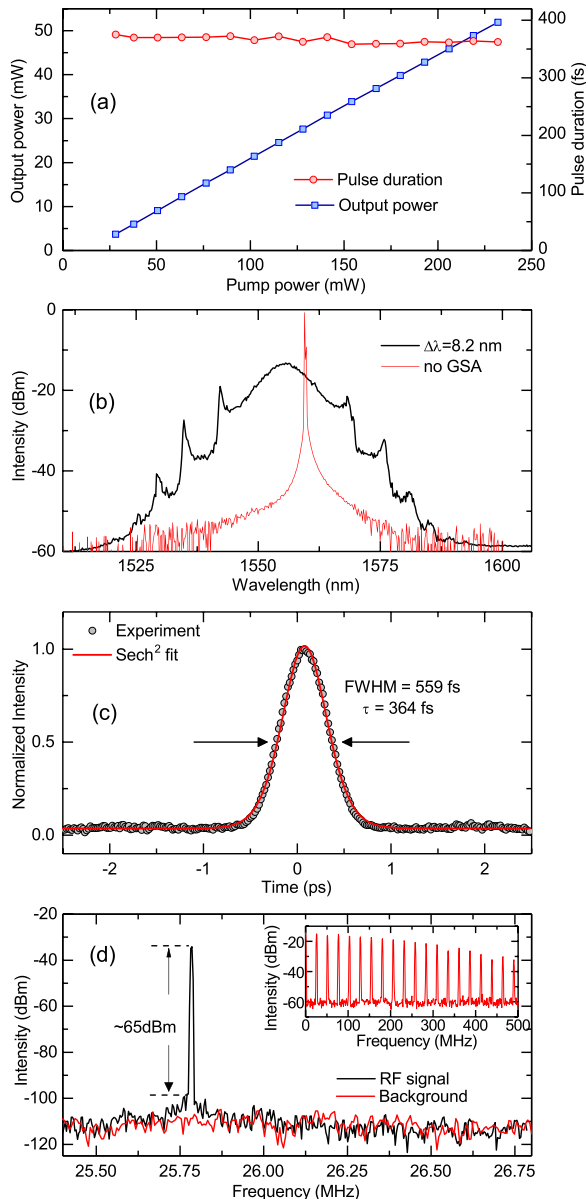


FIG. 3. (a) Scaling of output power and variation of pulse duration with pump power. Laser measurements recorded at maximum output power, showing (b) optical spectrum with ~ 1555 nm center wavelength and ~ 8.2 nm spectral width, with the red line indicating CW operation when the GSA is removed, (c) autocorrelation trace with pulse duration ~ 364 fs, and (d) first harmonic of the RF spectrum with ~ 65 dBm peak to pedestal extinction ratio. Inset: RF spectrum at maximum output power with 500 MHz span.

The radio frequency (RF) spectrum of the pulse train, measured with a photodetector connected to an RF spectrum analyzer, is reported in Fig. 3(d), for the first harmonic, 25.8 MHz, and up to 500 MHz. The fundamental repetition rate matches the cavity length, thus confirming single pulse operation. A signal-to-noise ratio ~ 65 dB indicates pulse stability up to the maximum output power. For $P_{out} = 52$ mW, the corresponding pulse energy is $E_c = 2$ nJ and the peak power $P_{peak} = 5$ kW. For higher P_{out} , i.e., increasing the pump power over 232 mW, pulse breaking is observed, which can be attributed to optical non-linearities in the fiber arising from high intra-cavity peak intensities.⁶³ Use of photonic crystal fibers with tailored nonlinearities¹⁰ could enable higher output powers which, combined with the broadband nature of graphene,³² could, in principle, extend our approach at other wavelengths.

Compared to Ti:Sa and OPOs, our all-fiber design, exploiting a GSA, is simpler to assemble, needing no critical alignment. A graphene-based all-fiber setup capable of $P_{out} \sim 15$ mW pulses at ~ 1560 nm was reported in Ref. 65. However, the use of a multilayer CVD graphene/polymethyl methacrylate structure complicates the fabrication process.⁶⁵ Reference 43 used a LPE based GSA to generate $P_{out} \sim 60$ mW at 1180 nm. Despite the higher P_{out} , the pulses were ~ 200 ns long, with lower $P_{peak} < 1$ W,⁴³ than the ~ 5 kW in our laser.

In conclusion, we demonstrated a mode-locked all-fiber laser with output power adjustable from 3.7 to 52 mW, using a graphene film as saturable absorber. The maximum pulse energy is $E_c = 2$ nJ corresponding to a $P_{peak} \sim 5$ kW, making it attractive for applications such as laser imaging.

We acknowledge funding from the EU Graphene Flagship, ERC Grants Hetero2D and HiGraphink, EPSRC Grant Nos. EP/K01711X/1, EP/K017144/1, and EP/N010345/1, Emmanuel College, Cambridge, and Trinity College, the Isaac Newton Trust.

¹M. E. Fermann, A. Galvanauskas, and G. Sucha, *Ultrafast Lasers: Technology and Applications* (CRC Press, 2002).

²F. Dausinger, F. Lichtner, and H. Lubatschowski, *Femtosecond Technology for Technical and Medical Applications* (Springer, Berlin, 2004).

³C. Krafft, I. W. Schie, T. Meyer, M. Schmitt, and J. Popp, *Chem. Soc. Rev.* **45**, 1819 (2016).

⁴N. Vogler, S. Heuke, T. W. Bocklitz, M. Schmitt, and J. Popp, *Annu. Rev. Anal. Chem.* **8**, 359 (2015).

⁵C. L. Evans and X. S. Xie, *Annu. Rev. Anal. Chem.* **1**, 883 (2008).

⁶W. F. Cheong, S. A. Pahl, and A. J. Welch, *IEEE J. Quantum Electron.* **26**, 2166 (1990).

⁷See <https://www.coherent.com/lasers/main/chameleon-family> for a commercially available tunable Ti:Sapphire ultrafast oscillator.

⁸M. E. Fermann and I. Hartl, *Nat. Photonics* **7**, 868 (2013).

⁹M. J. F. Digonnet, *Rare Earth Doped Fiber Lasers and Amplifiers* (Marcel Dekker, NY, USA, 1993).

¹⁰P. Russell, *Science* **299**, 358 (2003).

¹¹J. M. Dudley and J. R. Taylor, *Nat. Photonics* **3**, 85 (2009).

¹²T. Hasan, Z. Sun, F. Wang, F. Bonaccorso, P. H. Tan, A. G. Rozhin, and A. C. Ferrari, *Adv. Mater.* **21**, 3874 (2009).

¹³Z. Sun, T. Hasan, F. Torrisi, D. Popa, G. Privitera, F. Wang, F. Bonaccorso, D. M. Basko, and A. C. Ferrari, *ACS Nano* **4**, 803 (2010).

¹⁴S. Y. Set, H. Yaguchi, Y. Tanaka, and M. Jablonski, *IEEE J. Sel. Top. Quantum Electron.* **10**, 137 (2004).

¹⁵S. Y. Set, H. Yaguchi, Y. Tanaka, and M. Jablonski, *J. Lightwave Technol.* **22**, 51 (2004).

- ¹⁶S. Yamashita, Y. Inoue, S. Maruyama, Y. Murakami, H. Yaguchi, M. Jablonski, and S. Y. Set, *Opt. Lett.* **29**, 1581 (2004).
- ¹⁷F. Wang, A. G. Rozhin, V. Scardaci, Z. Sun, F. Hennrich, I. H. White, W. I. Milne, and A. C. Ferrari, *Nat. Nanotechnol.* **3**, 738 (2008).
- ¹⁸V. Scardaci, Z. P. Sun, F. Wang, A. G. Rozhin, T. Hasan, F. Hennrich, I. H. White, W. I. Milne, and A. C. Ferrari, *Adv. Mater.* **20**, 4040 (2008).
- ¹⁹D. Popa, Z. Sun, T. Hasan, W. Cho, F. Wang, F. Torrisi, and A. Ferrari, *Appl. Phys. Lett.* **101**, 153107 (2012).
- ²⁰R. Going, D. Popa, F. Torrisi, Z. Sun, T. Hasan, F. Wang, and A. C. Ferrari, *Physica E* **44**, 1078 (2012).
- ²¹Z. Zhang, D. Popa, V. J. Wittwer, S. Milana, T. Hasan, Z. Jiang, A. C. Ferrari, and F. Ö. Ilday, *Appl. Phys. Lett.* **107**, 241107 (2015).
- ²²D. G. Purdie, D. Popa, V. J. Wittwer, Z. Jiang, G. Bonacchini, F. Torrisi, S. Milana, E. Lidorikis, and A. C. Ferrari, *Appl. Phys. Lett.* **106**, 253101 (2015).
- ²³Y. Ren, G. Brown, R. Mary, G. Demetriou, D. Popa, F. Torrisi, A. C. Ferrari, F. Chen, and A. K. Kar, *IEEE J. Sel. Top. Quantum Electron.* **21**, 1602106 (2015).
- ²⁴R. Mary, G. Brown, S. J. Beecher, R. R. Thomson, D. Popa, Z. Sun, F. Torrisi, T. Hasan, S. Milana, F. Bonaccorso, A. C. Ferrari, and A. K. Kar, *Appl. Phys. Lett.* **103**, 221117 (2013).
- ²⁵C. E. S. Castellani, E. J. R. Kelleher, D. Popa, T. Hasan, Z. Sun, A. C. Ferrari, S. V. Popov, and J. R. Taylor, *Laser Phys. Lett.* **10**, 015101 (2013).
- ²⁶M. Zhang, E. J. R. Kelleher, T. H. Runcorn, V. M. Mashinsky, O. I. Medvedkov, E. M. Dianov, D. Popa, S. Milana, T. Hasan, Z. Sun, F. Bonaccorso, Z. Jiang, E. Flahaut, B. H. Chapman, A. C. Ferrari, S. V. Popov, and J. R. Taylor, *Opt. Express* **21**, 23261 (2013).
- ²⁷R. I. Woodward, E. J. R. Kelleher, D. Popa, T. Hasan, F. Bonaccorso, A. C. Ferrari, S. V. Popov, and J. R. Taylor, *IEEE Photonic Tech. Lett.* **26**, 1672 (2014).
- ²⁸D. Popa, Z. Sun, T. Hasan, F. Torrisi, F. Wang, and A. C. Ferrari, *Appl. Phys. Lett.* **98**, 073106 (2011).
- ²⁹F. Torrisi, D. Popa, S. Milana, Z. Jiang, T. Hasan, E. Lidorikis, and A. C. Ferrari, *Adv. Opt. Mater.* **4**, 1088 (2016).
- ³⁰Z. Sun, D. Popa, T. Hasan, F. Torrisi, F. Wang, E. J. R. Kelleher, J. C. Travers, V. Nicolosi, and A. C. Ferrari, *Nano Res.* **3**, 653 (2010).
- ³¹D. Popa, Z. Sun, F. Torrisi, T. Hasan, F. Wang, and A. C. Ferrari, *Appl. Phys. Lett.* **97**, 203106 (2010).
- ³²F. Bonaccorso, Z. Sun, T. Hasan, and A. C. Ferrari, *Nat. Photonics* **4**, 611 (2010).
- ³³D. Brida, A. Tomadin, C. Manzoni, Y. J. Kim, A. Lombardo, S. Milana, R. R. Nair, K. S. Novoselov, A. C. Ferrari, G. Cerullo, and M. Polini, *Nat. Commun.* **4**, 1987 (2013).
- ³⁴A. C. Ferrari, F. Bonaccorso, V. Falko, K. S. Novoselov, S. Roche, P. Boggild, S. Borini, F. Koppens, V. Palermo, N. Pugno *et al.*, *Nanoscale* **7**, 4598 (2015).
- ³⁵F. Bonaccorso, A. Lombardo, T. Hasan, Z. P. Sun, L. Colombo, and A. C. Ferrari, *Mater. Today* **15**, 564 (2012).
- ³⁶I. H. Baek, H. W. Lee, S. Bae, B. H. Hong, Y. H. Ahn, D.-I. Yeom, and F. Rotermund, *Appl. Phys. Express* **5**, 032701 (2012).
- ³⁷C. A. Zaugg, Z. Sun, V. J. Wittwer, D. Popa, S. Milana, T. S. Kulmala, R. S. Sundaram, M. Mangold, O. D. Sieber, M. Golling, Y. Lee, J. H. Ahn, A. C. Ferrari, and U. Keller, *Opt. Express* **21**, 31548 (2013).
- ³⁸R. Mary, S. J. Beecher, G. Brown, F. Torrisi, S. Milana, D. Popa, T. Hasan, Z. Sun, E. Lidorikis, S. Ohara, A. C. Ferrari, and A. K. Kar, *Opt. Express* **21**, 7943 (2013).
- ³⁹M. Zhang, E. J. R. Kelleher, F. Torrisi, Z. Sun, T. Hasan, D. Popa, F. Wang, A. C. Ferrari, S. V. Popov, and J. R. Taylor, *Opt. Express* **20**, 25077 (2012).
- ⁴⁰M. N. Cizmeciyan, J. W. Kim, S. Bae, B. H. Hong, F. Rotermund, and A. Sennaroglu, *Opt. Lett.* **38**, 341 (2013).
- ⁴¹G. Zhu, X. Zhu, F. Wang, S. Xu, Y. Li, X. Guo, K. Balakrishnan, R. A. Norwood, and N. Peyghambarian, *IEEE Photonic Tech. Lett.* **28**, 7 (2016).
- ⁴²Y. Hernandez, V. Nicolosi, M. Lotya, F. M. Blighe, Z. Y. Sun, S. De, I. T. McGovern, B. Holland, M. Byrne, Y. K. Gun'ko, J. J. Boland, P. Niraj, G. Duesberg, S. Krishnamurthy, R. Goodhue, J. Hutchison, V. Scardaci, A. C. Ferrari, and J. N. Coleman, *Nat. Nanotechnol.* **3**, 563 (2008).
- ⁴³L. Zhang, G. Wang, J. Hu, J. Wang, J. Fan, J. Wang, and Y. Feng, *IEEE Photonics J.* **4**, 1809 (2012).
- ⁴⁴Z. Jiang, G. E. Bonacchini, D. Popa, F. Torrisi, A. K. Ott, V. J. Wittwer, D. Purdie, and A. C. Ferrari, in *CLEO: 2014* (Optical Society of America, San Jose, California, 2014), p. JTu4A.67.
- ⁴⁵H. Jeong, S. Y. Choi, M. H. Kim, F. Rotermund, Y.-H. Cha, D.-Y. Jeong, S. B. Lee, K. Lee, and D.-I. Yeom, *Opt. Express* **24**, 14152 (2016).
- ⁴⁶J. Park, K. Park, D. Spoor, B. Hall, and Y.-W. Song, *Opt. Express* **23**, 7940 (2015).
- ⁴⁷J. Sotor, M. Pawliszewska, G. Sobon, P. Kaczmarek, A. Przewolka, I. Pasternak, H. Cajzl, P. Peterka, P. Honzátko, I. Kašík, W. Strupinski, and K. Abramski, *Opt. Lett.* **41**, 2592 (2016).
- ⁴⁸C. S. Young, J. Hwanseong, H. Byung Hee, R. Fabian, and Y. Dong-II, *Laser Phys. Lett.* **11**, 015101 (2014).
- ⁴⁹Z. Cheng, H. Li, H. Shi, J. Ren, Q.-H. Yang, and P. Wang, *Opt. Express* **23**, 7000 (2015).
- ⁵⁰S. Y. Choi, D. K. Cho, Y.-W. Song, K. Oh, K. Kim, F. Rotermund, and D.-I. Yeom, *Opt. Express* **20**, 5652 (2012).
- ⁵¹C. Mattevi, G. Eda, S. Agnoli, S. Miller, K. A. Mkhoyan, O. Celik, D. Mastrogiovanni, G. Granozzi, E. Garfunkel, and M. Chhowalla, *Adv. Funct. Mater.* **19**, 2577 (2009).
- ⁵²T. Hasan, F. Torrisi, Z. Sun, D. Popa, V. Nicolosi, G. Privitera, F. Bonaccorso, and A. C. Ferrari, *Phys. Status Solidi B* **247**, 2953 (2010).
- ⁵³A. C. Ferrari, J. C. Meyer, V. Scardaci, C. Casiraghi, M. Lazzeri, F. Mauri, S. Piscanec, D. Jiang, K. S. Novoselov, S. Roth, and A. K. Geim, *Phys. Rev. Lett.* **97**, 187401 (2006).
- ⁵⁴C. Casiraghi, A. Hartschuh, H. Qian, S. Piscanec, C. Georgi, A. Fasoli, K. S. Novoselov, D. M. Basko, and A. C. Ferrari, *Nano Lett.* **9**, 1433 (2009).
- ⁵⁵F. Torrisi, T. Hasan, W. Wu, Z. Sun, A. Lombardo, T. S. Kulmala, G.-W. Hsieh, S. Jung, F. Bonaccorso, P. J. Paul, D. Chu, and A. C. Ferrari, *ACS Nano* **6**, 2992 (2012).
- ⁵⁶A. C. Ferrari and J. Robertson, *Phys. Rev. B* **64**, 075414 (2001).
- ⁵⁷S. Latil, V. Meunier, and L. Henrard, *Phys. Rev. B* **76**, 201402 (2007).
- ⁵⁸V. G. Kravets, A. N. Grigorenko, R. R. Nair, P. Blake, S. Anissimova, K. S. Novoselov, and A. K. Geim, *Phys. Rev. B* **81**, 155413 (2010).
- ⁵⁹M. Born and E. Wolf, *Principles of Optics: Electromagnetic Theory of Propagation, Interference and Diffraction of Light* (Cambridge University Press, 1999).
- ⁶⁰A. Cabasse, G. Martel, and J. L. Oudar, *Opt. Express* **17**, 9537 (2009).
- ⁶¹W. Koechner, *Solid-State Laser Engineering* (Springer, 1999).
- ⁶²M. Currie, J. D. Caldwell, F. J. Bezares, J. Robinson, T. Anderson, H. Chun, and M. Tadjer, *Appl. Phys. Lett.* **99**, 211909 (2011).
- ⁶³G. P. Agrawal, *Applications of Nonlinear Fiber Optics* (Academic Press, London, 2001).
- ⁶⁴U. Keller, *Progress in Optics* (Elsevier, 2004), Vol. **46**, p. 1.
- ⁶⁵J. Tarka, J. Boguslawski, G. Sobon, I. Pasternak, A. Przewolka, W. Strupinski, J. Sotor, and K. M. Abramski, *IEEE J. Sel. Top. Quantum Electron.* **23**, 1100506 (2017).